

Original Research

Rosmarinic acid represses colitis-associated colon cancer: A pivotal involvement of the TLR4-mediated NF- κ B-STAT3 axis



Bo-Ram Jin ^a; Kyung-Sook Chung ^b;
Soonjae Hwang ^c; Sam Noh Hwang ^c; Ki-Jong Rhee ^c;
Minho Lee ^{a,1,*}; Hyo-Jin An ^{a,1,**}

^a Department of Pharmacology, College of Korean Medicine, Sangji University, Wonju-si, Gangwon-do, Korea

^b Department of Pharmaceutical Biochemistry, College of Pharmacy, Kyung Hee University, Seoul, Republic of Korea

^c Department of Biomedical Laboratory Science, College of Health Sciences, Yonsei University at Wonju, Wonju-si, Gangwon-do, Republic of Korea

^d Department of Life Science, Dongguk University-Seoul, Goyang-si, Gyeonggi-do, Republic of Korea

Abstract

Previously, we found that rosmarinic acid (RA) exerted anti-inflammatory activities in a dextran sulfate sodium (DSS)-induced colitis model. Here, we investigated the anti-tumor effects of RA on colitis-associated colon cancer (CAC) and the underlying molecular mechanisms. We established an azoxymethane (AOM)/DSS-induced CAC murine model for *in vivo* studies and used a conditioned media (CM) culture system *in vitro*. H&E staining, immunohistochemistry, western blot assay, enzyme-linked immunosorbent assay, molecular docking, co-immunoprecipitation, and immunofluorescence assay were utilized to investigate how RA prevented colorectal cancer. In the AOM/DSS-induced CAC murine model, RA significantly reduced colitis severity, inflammation-related protein expression, tumor incidence, and colorectal adenoma development. It significantly modulated toll-like receptor-4 (TLR4)-mediated nuclear factor-kappa B (NF- κ B) and signal transducer and activator of transcription 3 (STAT3) activation, thus attenuating the expression of anti-apoptotic factors, which mediate transcription factor-dependent tumor growth. *In vitro*, RA inhibited CM-induced TLR4 overexpression and competitively inhibited TLR4-myeloid differentiation factor 2 complex in an inflammatory microenvironment. Thus, RA suppressed NF- κ B and STAT3 activation in colon cancer cells in an inflammatory microenvironment. Therefore, RA suppressed colitis-associated tumorigenesis in the AOM/DSS-induced CAC murine model and abrogated human colon cancer progression in an inflammatory microenvironment by propitiating TLR4-mediated NF- κ B and STAT3 activation, pleiotropically.

Neoplasia (2021) 23, 561–573

Keywords: Colitis-associated colon cancer (CAC), Myeloid differentiation factor 2 (MD-2), Nuclear factor-kappa B (NF- κ B), Rosmarinic acid (RA), Signal transducer and activator of transcription 3 (STAT3), Toll-like receptor-4 (TLR4)

Introduction

Colorectal cancer (CRC) is one of the most commonly diagnosed cancers and the third leading cause of cancer-related mortality worldwide [1]. Conversion to malignancy is one of the main complications of inflammatory bowel disease (IBD), and the progression of cancer is associated with the severity, extent, and duration of IBD [2]. The cumulative possibility of CRC

Abbreviations: AOM, Azoxymethane; CPT, Camptothecin; CAC, Colitis-associated colon cancer; CRC, Colorectal cancer; DSS, Dextran sulfate sodium; IHC, Immunohistochemistry; IBD, Inflammatory bowel disease; NF- κ B, Nuclear factor-kappa B; RA, Rosmarinic acid; STAT3, Signal transducer and activator of transcription 3; TLR4, Toll-like receptor-4; UC, Ulcerative colitis.

* Corresponding author: Tel.: +82-31-631-5138 Mobile: +82-10-2024-5484

** Corresponding author: Tel.: +82-33-738-7503; Fax: +82-33-730-0679

E-mail addresses: Minho.Lee@dgu.edu (M. Lee), sangjipharm@gmail.com (H.-J. An).

¹ These authors contributed equally to this work

Received 1 February 2021; received in revised form 17 March 2021; accepted 3 May 2021

in ulcerative colitis (UC) patients has been noted to range from 2% after 10 y of the disease and up to 18% after 30 y of disease [3]. Meanwhile, the process of exploring new treatments for UC and UC-associated CRC is still impending. Hence, to further improve survival of patients and reduce disease severity, the development of novel drugs with high efficacy is warranted.

Previous studies have suggested that immune cells constitute up to 50% of the tumor load, with the main representatives being lymphocytes and macrophages [4]. In the cellular environment in which tumors exist, immune cells facilitate and accelerate tumor initiation, promotion, progression, and metastasis by releasing several cytokines, chemokines, and growth factors [5]. Here, we used experimental models available to address the effects of immune cells on colon cancer induction and found that inflammatory microenvironments could advance colon cancer via a novel pathway involving toll-like receptor-4 (TLR4)-mediated nuclear factor-kappa B (NF- κ B)/signal transducer and activator of transcription 3 (STAT3) activation, pleiotropically.

Enhanced TLR4 activation was confirmed in colon cancer patients with long-standing IBD, with TLR4 expression correlating with the degree of dysplasia [6]. TLR4 is well known to mediate the activation of the NF- κ B pathway through a signal transduction process involving the innate immune response. TLR4-mediated NF- κ B has been linked to improper immune development and inflammation-induced tumor initiation and development by controlling relevant factors [7]. In contrast, NF- κ B communicates with STAT3 at multiple points and thereby accelerates tumor-associated inflammation, subsequently encouraging tumor incidence, progression, and metastasis [8]. STAT3, which plays a clear role in the invasion of colitis-associated colon cancer (CAC), is also a target gene of the TLR4 signaling pathway and supports the connection between inflammation and tumor growth [9, 10].

Rosmarinic acid (RA) is a pharmacologically active compound that is found in some culinary herbs of the Labiatae family, such as *Rosmarinus officinalis* L., *Mentha* spp., *Origanum vulgare* L., and *Thymus vulgaris*. [11]. There has been an increasing interest in the biological efficacies of RA, including its antioxidant, anti-inflammatory, and anti-proliferative effects [12-14]. A study has reported that RA possesses anti-inflammatory property that is mediated via inhibiting the activity of enzymes such as lipoxygenase and cyclooxygenases (COX), inhibiting pro-inflammatory cytokines expression, and altering the complement cascade pathway [15]. Recently, we reported that RA ameliorates colonic inflammation in a dextran sulfate sodium (DSS)-induced colitis mouse model via the dual inhibition of NF- κ B and STAT3 activation [16]. In addition, a previous study revealed that RA possesses chemopreventive properties in 1,2-dimethylhydrazine (carcinogen)-induced CRC [17]. Unfortunately, none of these studies reported the exact mechanism of how RA prevents CRC. In addition, we hypothesized that the pharmacological efficacy of RA in the CAC animal model mimics known mechanisms underlying colitis and cancer in humans.

Hence, in this study, we aimed to experimentally investigate the anti-tumoral effects of RA in inflammation-associated CRC and to determine underlying molecular mechanisms involving the regulation of transcription factors in colon tissues.

Materials and methods

Chemicals and reagents

Primary antibodies for inducible nitric oxide synthase (iNOS) (sc-650), COX-2 (sc-1745), TLR4 (sc-293072), STAT3 (sc-482), I κ B- α (sc-203), cyclin D1 (sc-753), β -actin (sc-81178), C23 (sc-8031), α -tubulin (sc-8035), survivin (sc-17779), XIAP (sc-55552), Bcl-2 (sc-7382), Bcl-xl (sc-8392), and Cdk-4 (sc-23896) were acquired from Santa Cruz (TX, USA). Moreover, p65 (#4764), pI κ B- α (#9246), p-STAT3 Ser727 (#9134), and p-STAT3 Tyr705 (#9145) were acquired from Cell Signaling (MA, USA). RPMI 1640, fetal

bovine serum (FBS), and penicillin were obtained from Gibco (MA, USA). Azoxymethane (AOM), 5-aminosalicylic acid (5-ASA), camptothecin (CPT), RA, AG 490, and all other chemicals were acquired from Sigma Aldrich (MO, USA).

Experimental animals and sample treatment

Male Balb/c mice (n = 55; 8 weeks old; 18-20 g) were obtained from Daehan Biolink Co. (Daejeon, Korea). All animal housing conditions, and experimental protocols were recognized by the Institutional Animal Care and Use Committee of Sangji University (#2016-12). Using a blinded method, animals were randomly distributed into 5 groups (n = 11): the control group; AOM/DSS group (constituting AOM/DSS-induced CAC mice); 5-ASA group (constituting AOM/DSS-induced CAC mice administered 5-ASA 75 mg kg⁻¹/day; orally); CPT group (constituting AOM/DSS-induced CAC mice administered CPT 0.5 mg kg⁻¹/day; intraperitoneally); and the RA 30 group (constituting AOM/DSS-induced CAC mice administered RA 30 mg kg⁻¹/day; orally). On day 14, DSS treatment was discontinued and ASA, CPT, or RA was administered to the mice every day for a week. As positive controls, we used 5-ASA, which is used to treat IBD, and CPT, an anticancer drug that inhibits DNA topoisomerase I. For further analysis, we removed three mice from each group, to consider death during survival tests.

Induction of CAC model

To establish the CAC model, each animal was intraperitoneally injected with 12.5 mg kg⁻¹ of AOM dissolved in phosphate-buffered saline (PBS). After 7 d, the animals were supplied drinking water containing 1% DSS for 7 d, followed by drinking water for 14 d, and then exposed to 2 more 2% DSS treatment cycles. This resulted in a total of 14 additional d of DSS treatment in addition to the first 7 at 1% DSS. Mice were weighed weekly and sacrificed on day 56.

Histopathology

The segregated colon samples were fixed instantly with 10% formalin and embedded in paraffin. The embedded samples were sectioned to 5- μ m slices and stained with hematoxylin and eosin (H&E) and periodic acid-Schiff, as described previously [18]. For histopathological analysis, the description of parameters used to score hyperplasia and inflammation degrees is presented in Tables 1 and 2, respectively.

Immunohistochemistry (IHC)

IHC was performed using formalin-fixed, paraffin-embedded samples. Paraffin blocks were cut into 5- μ m thick sections, mounted onto poly-L-lysine-coated slides, and dried. After the dried slides were de-paraffinized, antigen retrieval was performed using an automated antigen retrieval machine for 20 min with cell conditions of ethylenediaminetetraacetic acid (pH 9.0). Non-specific binding to the sections was blocked by incubating for 1 h in 15% to 20% normal goat serum (Gibco Life Technologies, NY, USA), prior to incubation with the appropriate primary antibodies for 2 h at room temperature (22-25°C) or overnight at 4°C. Secondary rabbit antibodies were used to detect the primary antibodies, followed by detection using streptavidin-tagged horseradish peroxidase (Ventana Medical Systems, Tucson, USA). Diaminobenzidine (Sigma Aldrich, St. Louis, MI, USA) was used to induce signaling, and Bluing Reagent (Ventana Medical Systems, Tucson, USA) was used as a counterstain. The IHC slides were visualized using an optical microscope (Leica, Wetzlar, Germany) and rendered using the Leica software. IHC staining of antibodies against TLR4 (sc-293072, Santa Cruz), NF- κ B p65 (#4764, Cell Signaling), and p-STAT3 Tyr705

Table 1

Score of histopathological hyperplasia.

Histological Parameters		
Mucosa	Description	Score
Non-dysplastic Epithelium	Mild (less than twofold) crypt length	1
	Intense crypt length with hyperchromatic CEC	2
Dysplastic Epithelium	Dysplastic epithelial region (legion < 20%)	1
	Dysplastic epithelial region (20% < legion < 50%)	2
	Dysplastic epithelial region (50% < legion < 90%)	4

Table 2

Score of histopathological inflammation.

Histological Parameters		
Mucosa	Description	Score
Epithelial cell	Prolonged epithelial cell or crypt	1
	Destruction of barrier	2
	Ulcer (30% < loss < 60%)	3
	Ulcer (loss > 60%)	4
Immune cell	Infiltration (mild)	1
	Infiltration (moderate)	2
	Infiltration (severe)	3
Submucosa Immune cell	Infiltration (mild)	1
	Infiltration (moderate)	2
	Infiltration (severe)	3

Table 3

Score of Immune-reactivity.

Description	Score
Mild	1
Moderate	2
Intense	3
Severe	4

(#9145, Cell Signaling) was examined. Immunoreactivity score of TLR4, NF- κ B p65 and p-STAT3 Tyr705 was assessed in the representative pictures of each group according to Table 3.

Western blot analysis

Protein was extracted from mice colon tissues and human colon cancer cells utilizing the protein lysis buffer (Pro-prep, Intron, Seongnam, Korea). Nuclear extraction was conducted as described previously [19]. Quantified samples were fractioned on an 8-12% gradient sodium dodecyl sulfate (SDS) gel, transferred to PVDF membranes, and then probed with specific primary antibodies in T-TBS (2.5% skim milk) at 4°C. Peroxidase-conjugated secondary antibodies (Jackson ImmunoResearch, PA, USA) were incubated at 25°C. Subsequently, bands were visualized using an ECL solution (Ab signal, Seoul, Korea) and manifested on an X-ray film (Agfa, Belgium).

Enzyme-linked immunosorbent assay (ELISA)

Protein extraction from the mice colon tissues was performed to determine the level of IL-6 using a BD OptEIA mouse IL-6 ELISA Set (#555240, BD BioSciences, CA, USA). Aliquots of each protein sample (30 μ g) were diluted

in Reagent Diluent (Cat No: 555213). The experiments were performed according to the manufacturer's instructions.

Molecular docking

To predict the binding mode of RA on TLR4, molecular docking was conducted using AutoDock Vina [20]. The previously determined X-ray structure (PDB ID: 2Z63) of TLR4 was used [21]. All hetero atoms including water molecules were removed before docking. The structure of RA was downloaded from PubChem (CID: 5281792). The value of exhaustiveness in AutoDock Vina was set to 40. RA-bound structure of TLR4 was visualized and analyzed by PyMol [22], and two-dimensional interactions between RA and TLR4 were estimated using LigPlot+ [23].

Cell culture and conditioned media (CM) culture

The human colorectal carcinoma cell line HCT116 (lines < 15), the human colorectal adenocarcinoma cell line HT29 (lines < 15), and the human monocyte cell line THP-1 (lines < 8) were obtained from the Korean Cell Line Bank (Seoul, Korea). HCT116, HT29, and THP-1 cells were cultured in RPMI 1640 media supplemented with 10% FBS, 100 U/ml penicillin, and 100 mg/ml streptomycin. Cells were cultured in a humidified environment with 5% CO₂ at 37°C. Next, 100 ng/ml phorbol 12-myristate 13-acetate (PMA) was added to the THP-1 cells for 48 h, after which the supernatant was collected following centrifugation at 4000 rpm/min for 10 min. Colon cancer cells were treated with CM with or without RA and AG 490 for 30 min.

Cell viability assay

Cells were treated with RA (0-200 μ M) and incubated overnight. Next, MTT solution (5 mg/ml) was added for 2 h. After soaking the supernatant, the formazan product was dissolved in dimethyl sulfoxide, and the extent of cytotoxicity was measured at 570 nm using a BioTek Epoch microplate spectrophotometer (VT, USA). Experiments were performed in triplicate in a parallel manner, and the values were represented as means \pm standard deviations (SDs).

Co-immunoprecipitation

In vitro binding of TLR4 and myeloid differentiation factor 2 (MD-2) using protein A/G mix magnetic beads (Thermo Scientific, MA, USA) was performed as described by the manufacturer. Beads were washed three times and bound to anti-TLR4 and IgG on a tumbling wheel at 20°C for 2 h. Meanwhile, HT29 and HCT116 cells were treated with CM with or without RA for 30 min. Colon cancer cells were harvested by scraping, and cell lysis was performed through sonication of cells in a lysis buffer that contained 0.5% NP-40 and a protease inhibitor cocktail. Protein concentration in the cell lysate was determined, and 500 μ g of the protein was then used for the

reaction. Protein was incubated with antibody-bound beads on a tumbling wheel at 4°C overnight, and the proteins bound to anti-TLR4 and IgG were eluted with 50 µL of 0.5 M glycine (pH 3.5) and resolved using 10% SDS-PAGE gel for western blot analysis.

Immunofluorescence

After the indicated treatments were completed, HT29 and HCT116 cells were fixed in 100% methanol for 30 min at room temperature. The cells were then blocked with 10% normal goat serum (Gibco) for 1 h at room temperature. The cells were then incubated with primary antibodies for TLR4, NF-κB p65, and pSTAT3 Tyr705 overnight at 4°C. After washing with PBS and 0.3% Triton X, the cells were incubated for 1 h with anti-rabbit IgG secondary antibody conjugated with Alexa Fluor 488. Then, the nuclei were counterstained with 4',6-diamidino-2-phenylindole (Life Technologies, CA, USA). Conjugated proteins were detected using optical microscopy (ECLIPSE Ni-U, Nikon, Tokyo, Japan).

Statistical analysis

Experiments were performed in triplicate, and data were expressed as means ± SDs. Statistically significant values were determined using an analysis of variance and Dunnett's post hoc test. *P*-values < 0.05 were considered statistically significant. Statistical analysis was performed using GraphPad Prism 5.

Results

RA ameliorated pathological symptoms in the AOM/DSS-induced CAC mouse model

As shown in Figure 1B, 5-ASA, CPT, and RA treatments notably augmented the survival of AOM/DSS-induced CAC mice during the experimental period. Symptomatic factors of colitis, including proctorrhagia and severe diarrhea, were detected in the AOM/DSS group. There was no significant difference in the total body weight between each experimental group following treatment termination (day 56), whereas the body weight in the AOM/DSS group was dramatically decreased after AOM injection (Fig. 1C). The colon length in the AOM/DSS group was dramatically shortened than that in the control group, but the administration of 5-ASA, CPT, and RA restored the colon length (Fig. 1D). The colon length in the AOM/DSS group was -1.6-fold lower compared with that of the control group. In the 5-ASA, CPT, and RA groups, the colon lengths were -1.2-, -0.9 and -0.9-fold lower, respectively, compared with the control group. Furthermore, spleen enlargement was observed in AOM/DSS-treated mice, but 5-ASA, CPT, and RA treatments significantly reduced splenic enlargement (Fig. 1E).

RA attenuated tumorigenesis in the AOM/DSS-induced CAC mouse model

The combination of a single mutagenic AOM treatment and several DSS cycles resulted in an aberrant crypt foci (ACF)-adenoma-carcinoma sequence that closely mirrored the pattern seen in humans [24]. As shown Figure 1F, polypoid tumors were found in the middle and terminal parts of the colon in AOM/DSS-treated mice, but 5-ASA, CPT, and RA treatments significantly decreased the tumor mass in AOM/DSS-treated mice. Tumor multiplicity, indicating the total number of macroscopic lesions per mouse, in the AOM/DSS group was 29 and in the 5-ASA, CPT, and RA groups they were 12, 8, and 5, respectively. Figure 2A and Table 4 show the H&E-stained histological sections in each group and histological parameters of the

Table 4

Histological parameters of distal colon for assessment of neoplasia.

Group	Aberrant Crypt foci (ACF) (%)	Microadenoma (%)	Low-Grade Macroadenoma (%)	High-Grade Macroadenoma (%)	Adenocarcinoma (%)
CON	0.00%	0.00%	0.00%	0.00%	0.00%
AOM/DSS	37.84%	29.73%	21.62%	8.11%	2.70%
5-ASA	95.45%	0.00%	4.55%	0.00%	0.00%
CPT	42.86%	28.57%	21.43%	14.29%	0.00%
RA	55.56%	27.78%	16.67%	0.00%	0.00%

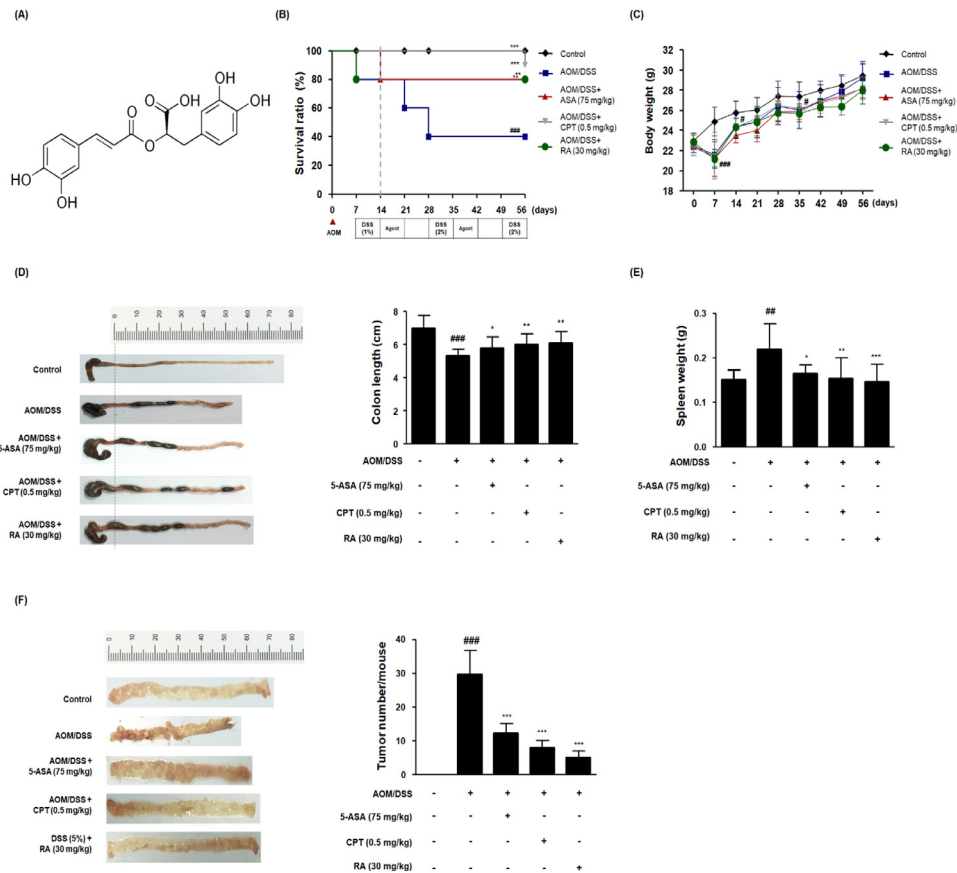


Fig. 1. Effects of RA on the development of the AOM/DSS-induced CAC *in vivo* model. (A) Molecular structure of RA. (B) Kaplan–Meier survival analysis shows the effect of RA on the survival ratio of AOM/DSS-induced CAC mice. (C) Body weight was evaluated every week during the experimental period. (D) A representative appearance and data statistics of colon length is presented. The length of the colon of each animal was measured between the caecum and proximal rectum. (E) The spleen was weighed in each experimental group. (F) Using a blinded method, all tumor masses in each colonic tissue were numbered and the mean values were calculated for each group. Numerical values are presented as means \pm standard deviations ($n = 8$); # $P < 0.05$, ## $P < 0.01$, ### $P < 0.001$ when compared with the control group; * $P < 0.05$, ** $P < 0.01$, *** $P < 0.001$ when compared with the AOM/DSS-induced CAC group; significances between each experimental group were determined by analysis of variance and Dunnett's post hoc test.

distal colon for the assessment of neoplasms, respectively. Upon histological evaluation of the tumor, we found no metastatic cancers in any tissues, such as liver, of AOM/DSS-treated mice. In AOM/DSS-treated mice, 37.84% of the lesions were ACF, 29.73% were microadenomas, and 2.7% were adenocarcinomas. In contrast, in 5-ASA-, CPT-, and RA-treated mice, no adenocarcinomas were noted. In the 5-ASA and RA 30 groups, almost all lesions were low-grade ACF and microadenomas. Taken together, these results demonstrated that RA as well as ASA may have therapeutic effects in AOM/DSS-treated CAC mice.

RA inhibited inflammatory markers in the AOM/DSS-induced CAC mouse model

To investigate the involvement of chronic inflammation in AOM/DSS-treated mice, we performed H&E staining and characterized pathological findings. As demonstrated in Figure 2A, AOM/DSS-treated mice showed severe distortion of barriers and infiltration of immune cells. However, treatment with 5-ASA, CPT, and RA inhibited the augmentation of crypt distortion and restricted mucosal and submucosal infiltrations. Unlike the control group, the AOM/DSS group had significantly elevated muscle thickness in the colon, which was used to examine inflammation in the intestinal tract [25]. However, 5-ASA, CPT, and RA treatments decreased colonic muscle thickness (Fig. 2D). In addition, we investigated the

effects of RA on representative inflammatory markers *in vivo*. Compared with AOM/DSS administration, 5-ASA, CPT, and RA administration significantly inhibited COX-2 and iNOS protein levels (Fig. 2E). As shown in Figure 2F, we also observed that AOM/DSS increased the level of IL-6, an inflammation/cancer-related marker and a common activator of NF- κ B and STAT3, whereas RA inhibited the production of IL-6.

RA suppressed NF- κ B activation and NF- κ B-related protein expression in the AOM/DSS-induced CAC mouse model

To elucidate the molecular mechanism of RA, we evaluated the effects of RA on NF- κ B activation in the AOM/DSS-induced CAC mouse model. As shown in Figure 3A, the AOM/DSS group demonstrated a marked difference compared with the control group. However, RA inhibited the protein expression of NF- κ B p65 in the tumor tissues of AOM/DSS-induced CAC mice. Consistently, the AOM/DSS group exhibited an increased translocation of p65, and RA inhibited the nuclear p65 protein expression, as confirmed by western blot analysis. We also found that RA suppressed the phosphorylation and degradation of I κ B and decreased the protein levels of survivin, Bcl-2, Bcl-xl, and XIAP (Fig. 3B and 3C).

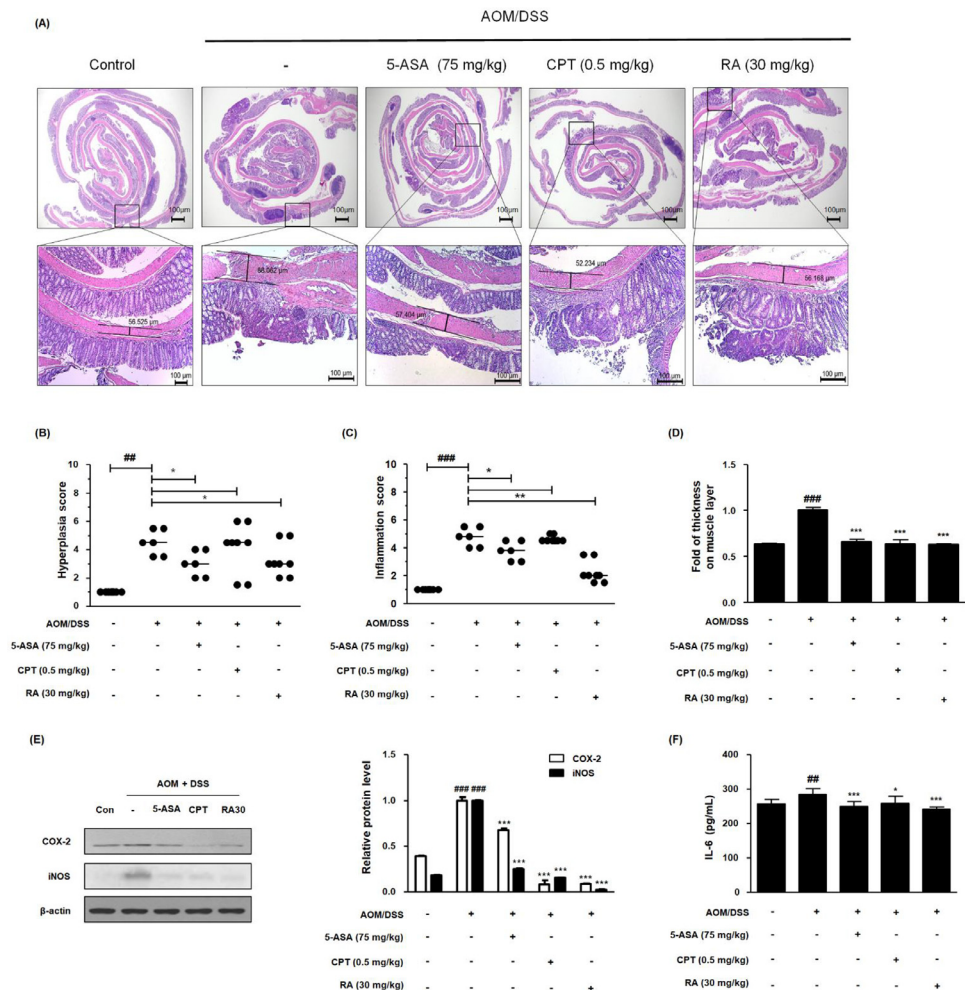


Fig. 2. Effect of RA on the inflammatory response in the AOM/DSS-induced CAC *in vivo* model. (A) Whole colonic tissues were stained using H&E. (B) The hyperplasia score and (C) inflammation score in AOM/DSS-induced CAC mice were estimated. (D) Colonic muscle thickness was determined using the LAS software. Slide sections were scrutinized by microscopy. Magnification $\times 40$ and $\times 100$ inset. (E) The expression of COX-2 and iNOS was estimated by western blotting in triplicate, and relative protein level was measured by densitometric analysis using Image J. (F) Production of IL-6 was determined using an ELISA kit. Values are means \pm standard deviations ($n = 8$); $^{##}P < 0.01$, $^{###}P < 0.001$ compared with the control group; $^{*}P < 0.05$, $^{**}P < 0.01$, $^{***}P < 0.001$ compared with the AOM/DSS-induced CAC group; significances between treated groups were determined by analysis of variance and Dunnett's post hoc test.

RA reduced STAT3 activation and STAT3-related protein expression in the AOM/DSS-induced CAC mouse model

IHC analysis revealed strong expression of pSTAT3 Tyr705 in the colon of AOM/DSS-induced CAC mice. However, 5-ASA and RA significantly reduced the levels of pSTAT3 Tyr705 (Fig. 4A). Similarly, western blot analysis showed that unlike the control group, the AOM/DSS group showed increased expression of pSTAT3 Tyr705 and Ser727. Meanwhile, it was confirmed that there was no change in the total expression of STAT3. As shown in Figure 4B and 4C, we observed that 5-ASA, CPT, and RA treatments suppressed the phosphorylation of STAT3 at the Tyr705 and Ser727 residues in colonic protein extracts. In addition, 5-ASA, CPT, and RA treatments abrogated nuclear translocation of pSTAT3 Tyr705 and overexpression of STAT3 target genes, including Cdk4 and cyclin D1.

RA obliterated TLR4 expression in the AOM/DSS-induced CAC mouse model

Progressively activated TLR4 encourages the proliferation of colon cancer cells and extricates cancer cells from death [26, 27]. As shown in Figure 5A,

AOM/DSS immunostaining showed the highest level of TLR4 in colon tissue. However, we found that the TLR4 level following 5-ASA, CPT, and RA treatments was significantly lower than that following the AOM/DSS treatment. We also demonstrated that AOM/DSS increased the protein expression of TLR4, whereas 5-ASA, CPT, and RA treatments inhibited the overexpression of TLR4 (Fig. 5B).

RA is predicted to bind to TLR4 Arg-264 domain by computational docking

Synthetic or natural antagonists of TLR4 can block TLR4 signaling by interacting with the TLR4-myeloid differentiation factor 2 (MD-2) complex, thus competing with the recognition of lipopolysaccharide (LPS) [28]. We performed a structure-based molecular docking study for the identification of interactions between RA and TLR4. Molecular docking results suggested that RA interacted with TLR4, indicating the competitive inhibition of the TLR4-MD-2 complex. Arg-264 of the TLR4 region was the predominant residue binding to RA (Fig. 5C).

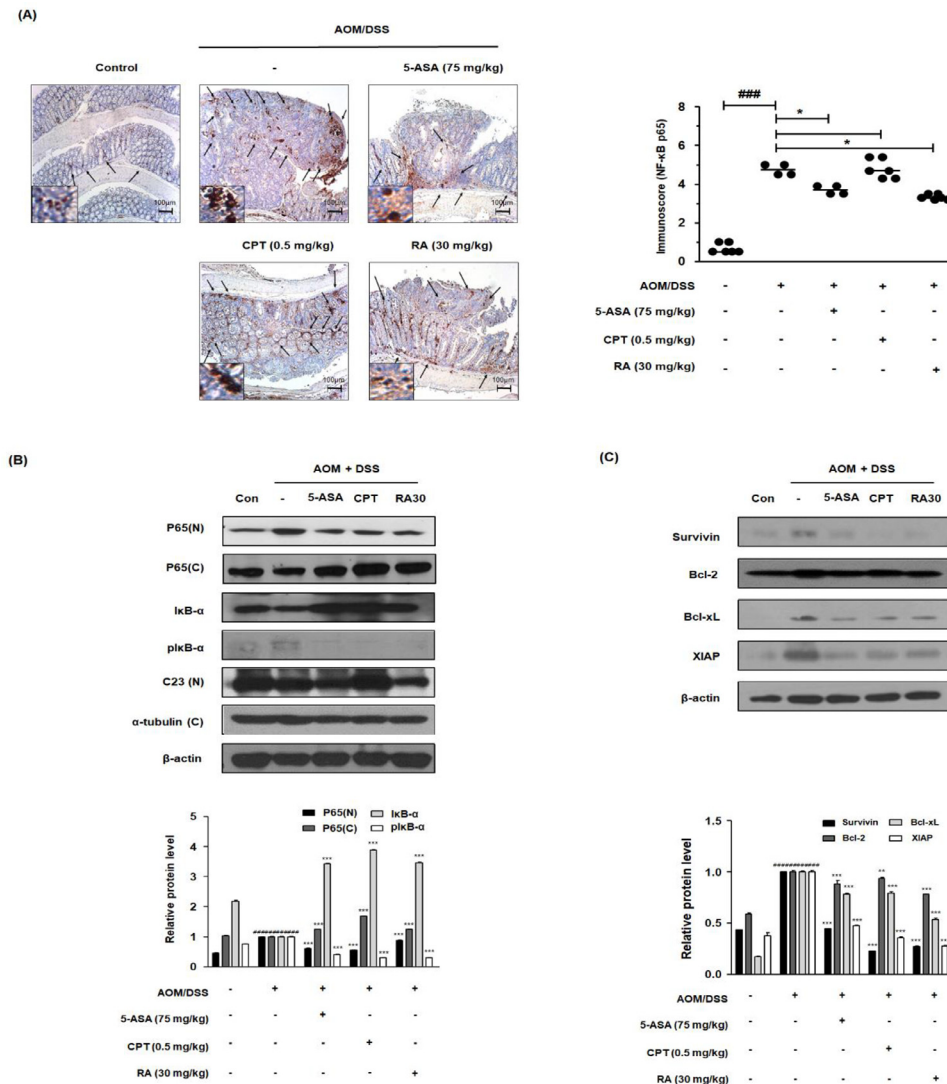


Fig. 3. Effect of RA on NF- κ B activation and its relative proteins in the AOM/DSS-induced CAC *in vivo* model. (A) The nuclear manifestation and translocation of NF- κ B p65 in colon tissues were observed using IHC. Immunoscore of NF- κ B p65 in the colon of AOM/DSS-induced mice was estimated. (B) Nuclear (N) and cytosolic (C) extracts were prepared from colon tissues. NF- κ B p65 translocation to the nucleus and phosphorylation of I κ B were estimated by western blotting in triplicate. (C) The expression of NF- κ B-related proteins was determined by western blotting in triplicate. C23, α -tubulin, and β -actin were used as internal controls. The relative ratio level was normalized to internal controls and determined by densitometric analysis. Values are presented as means \pm standard deviations ($n = 8$); $### P < 0.001$ vs the control group; $*P < 0.05$, $**P < 0.01$, $***P < 0.001$ vs the AOM/DSS-induced CAC group; significances between treated groups were determined using an analysis of variance and Dunnett's post hoc test.

RA restrained the overexpression of TLR4, and binding of the TLR4-MD-2 complex stimulated by CM in human colon cancer cells

As shown in Figure 6A and 6B, treatment with RA (6.25–200 μ M) had no effect on the viability of HCT116 and HT29 cell lines. Accordingly, we investigated the molecular effects of RA on inflammation-related colon cancer cell progression. Immunofluorescence analysis confirmed that CM stimulation induced the overexpression of TLR4 as much as LPS treatment. However, treatment with 25 and 50 μ M RA notably inhibited these effects of CM stimulation in HCT116 and HT29 cell lines (Fig. 6C and 6D). Next, we identified interactions between RA and TLR4 in inflammation-related colon cancer cells using co-immunoprecipitation. The results showed that RA competitively inhibited the binding of the TLR4 and MD-2 complex in the HCT116 and HT29 cell lines (Fig. 6E).

RA inhibited CM-mediated NF- κ B activation in human colon cancer cells

Figure 6 shows the inhibitory effects of RA on the activation of TLR4 in HCT116 and HT29 cells exposed to inflammatory microenvironments. Next, the effect of RA on the downstream TLR4 signaling in CM-stimulated colon cancer cells was investigated. The results indicated that CM from the PMA-stimulated THP-1 environment enhanced nuclear translocation of NF- κ B in HCT116 and HT29 cells. As shown in Figure 7A and 7B, RA and AG490 Janus Kinase 2-specific inhibitor suppressed NF- κ B nuclear translocation unlike that observed in the control group treated with CM. The immunofluorescence assay revealed that the activation of NF- κ B significantly increased under CM stimulation-inducing conditions than that under control conditions, whereas RA suppressed the overexpression of translocation of NF- κ B subunit p65 in a concentration-dependent manner (Fig. 7C and 7D).

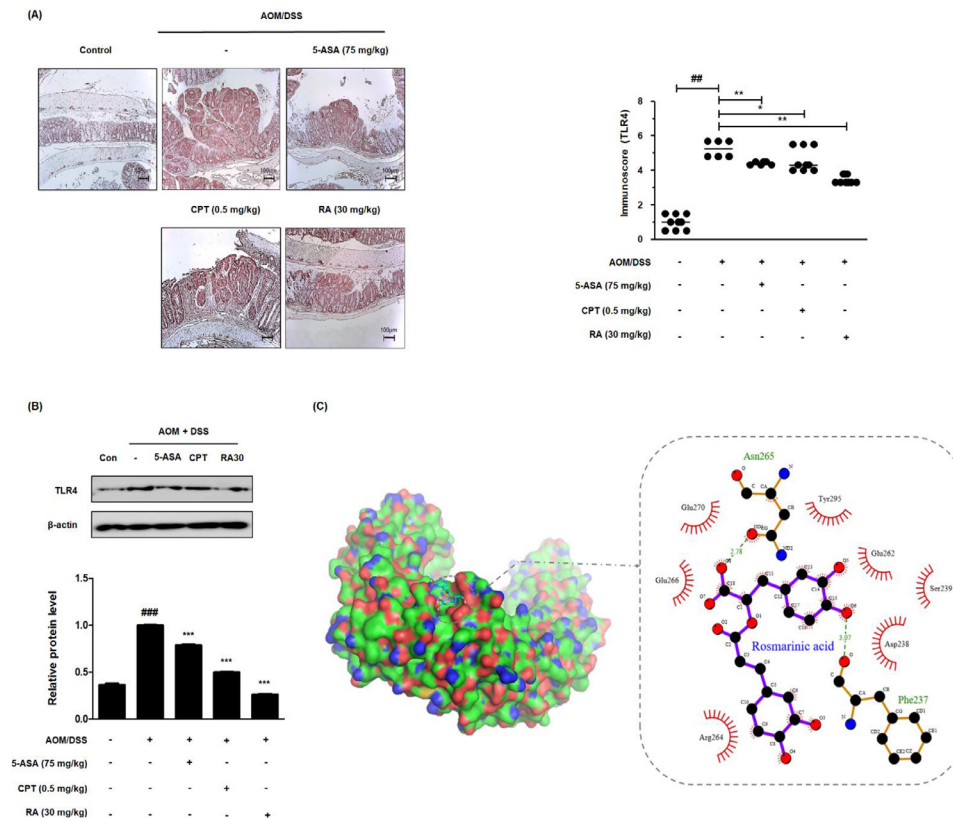


Fig. 5. Effect of RA on TLR4 in the AOM/DSS-induced CAC *in vivo* model and molecular docking for the binding of RA to TLR4. (A) The expression of TLR4 in colon tissues of AOM/DSS-induced mice was identified using IHC. Immunoreactivity of TLR4 was assessed based on stained slides. (B) The expression of TLR4 in AOM/DSS-induced CAC mice colon tissue was estimated by western blotting in triplicate. Values are the means \pm standard deviations ($n = 8$); $##P < 0.01$, $###P < 0.001$ vs the control group; $*P < 0.05$, $**P < 0.01$, $***P < 0.001$ vs the AOM/DSS-induced CAC group; significances between treated groups were determined using an analysis of variance and Dunnett's post hoc test. (C) Molecular docking simulation was conducted to determine whether RA binds to TLR4 using the AutoDock Vina program.

Furthermore, this finding provides evidence that the administration of 5-ASA may lead to the prevention of UC progressing into CRC [35]. These reports suggest the involvement of inflammation in the carcinogenic pathway and represent a promising approach in the development of anti-inflammatory drugs for cancer prevention and therapeutics. Meanwhile, 5-ASA can have undesirable and serious adverse effects, including headache, stomachache, and allergic reactions [36].

Chemotherapy is a regimented cancer treatment and is one of the most commonly used treatments for advanced-stage CRC. Some common drugs used for CRC include 5-fluorouracil, capecitabine, and the CPT analog irinotecan. The use of chemotherapeutic agents is often associated with poor response rates, unfavorable side effects, and cytotoxicity. Chemotherapy induces damage in rapidly dividing cells and unfortunately does not distinguish between normal cells and tumor cells. Therefore, it is imperative to develop novel chemotherapeutic agents with low risks and toxicities [37–39].

This study was designed to determine the protective efficacy of RA in an AOM/DSS-induced CAC murine model. This model strengthens the hypothesis that inflammation plays a critical role in IBD-related colon carcinogenesis [40]. In inflammatory and/or carcinogenic environments, various molecular signals are likely to play a pivotal role, including overexpression of cytokine and chemokine by immune cells, which advance the probability of mutagenesis and the crosstalk between cancer cells and surrounding lesions [41].

A large body of evidence suggests that tumor cell apoptosis occurs concomitantly with the inhibition of NF- κ B, and in the present study, we found that RA treatment regulated the anti-apoptotic NF- κ B target proteins, including survivin, Bcl-2, Bcl-xL, and XIAP. It is remarkable that the complex formation of survivin and XIAP activates NF- κ B, and the activation of NF- κ B in turn promotes the expression of survivin [42]. XIAP is the best characterized IAP regulated by NF- κ B and directly inhibits caspase-3 and caspase-9 [43]. NF- κ B also inhibits apoptosis via the mitochondrion-dependent pathway, and this activity could be mediated through the Bcl-2 family members, such as Bcl-xL. Bcl-2, known as the most potent anti-apoptotic members, is classified as an oncogene [44].

Quenching cell proliferation by the suppression of the IL-6/JAK/STAT3 pathway has been considered as a potential therapeutic strategy in the treatment of CRC [45]. The activation of STAT3 has been closely associated with cell growth, survival, and differentiation of relative proteins, such as cyclin D and Cdk4. In tumor-suppressor genes that fail to express STAT3 or those that are mutated, cyclin D1, which appears to form a complex with CDK4, results in the abnormal stimulation of cell division and undisciplined cell growth or tumor development [46].

The intestinal epithelium is continually exposed to gram-negative bacterial LPS. Recognition of LPS by TLR4 is implicated in the inflammatory responses in intestinal epithelial cells and mediates the development of colitis-associated tumorigenesis by mechanisms including the secretion of cytokines and a direct recruitment of NF- κ B [47, 48]. Reports have also highlighted the crosstalk between TLR4/NF- κ B pathways and IL-

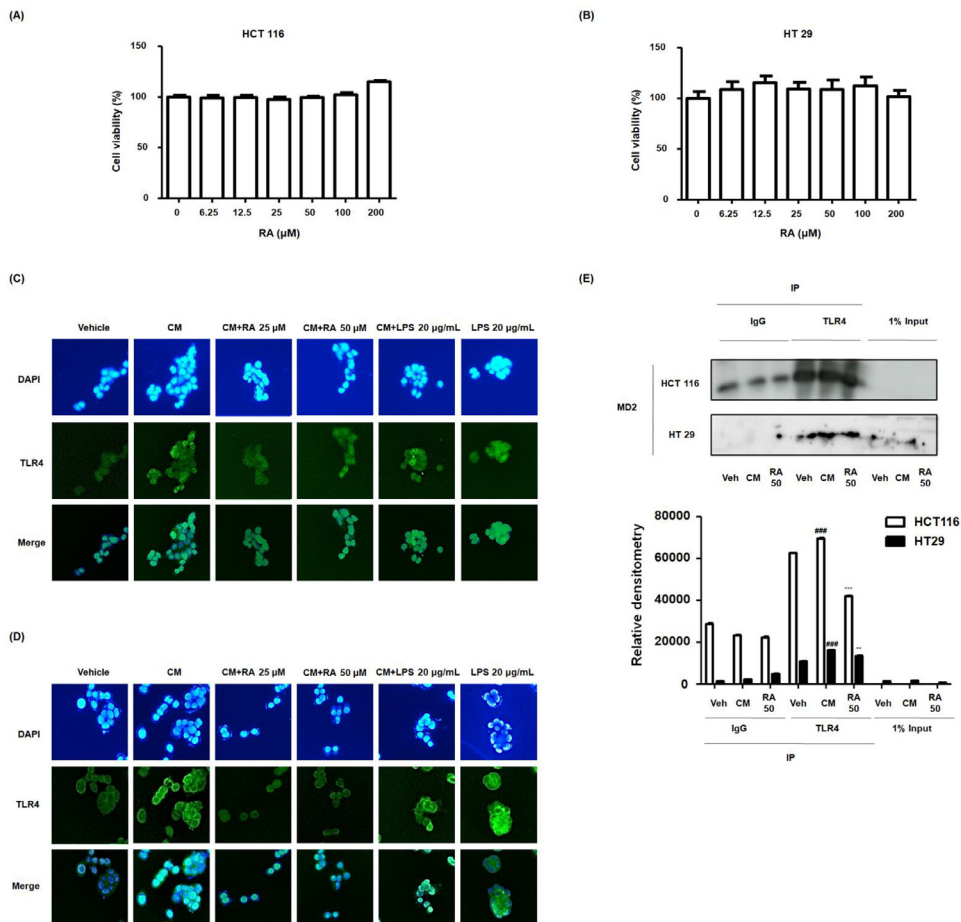


Fig. 6. Effect of RA on binding of TLR4-MD-2 complex in human colon cancer cells exposed to inflammatory microenvironments. (A) MTT assay was used to detect the cytotoxic effect of RA on HCT116 and HT29 cells. Experiments were performed in triplicate in a parallel manner, and the values were represented as means ± standard deviations. (C-E) Every group was treated with CM. In the conditioned culture system, the ratio of the colon cancer cell media to the THP-1 supernatant was 1:5. The vehicle and LPS 20 μg/mL groups were treated with CM from the nonstimulated THP-1 cell, and received no treatment or were treated with LPS 20 μg/mL. The cells exposed to CM from PMA-activated THP-1 cells received no treatment or were treated with 25, 50 μM RA or 20 μg/mL LPS. Then, the cells were further incubated for 5 min. (C-D) Immunofluorescence staining of TLR4 (green) and 4’6-diamidino-2-phenylindole (DAPI; blue) in CM-treated (C) HCT116 cells and (D) HT29 cells. LPS was used as a positive control to evaluate the effects of CM on HT29 and HCT116 cells via TLR-4 mediated NF-κB/STAT3 pathways. (E) Binding activity of TLR4 and MD-2 complexes was analyzed using HT 29 and HCT116 cell lysates using co-immunoprecipitation in triplicate. Values are presented as means ± standard deviations; ###*P* < 0.001 vs Veh (Vehicle) group where TLR4 was pulled down from cancer cell; ***P* < 0.01 and ****P* < 0.001 vs CM group where TLR4 was pulled down from cancer cell; significances between groups were determined by analysis of variance and Dunnett’s post hoc test.

6-dependent JAK/STAT3 as a potential mechanism in LPS-driven pro-inflammatory responses, whereby these signaling pathways regulate the severity of the host inflammatory response [49]. Meanwhile, it has been recently demonstrated that TLRs, and particularly TLR4, are involved in noninfectious diseases. TLR4 engagement by endogenous ligands has been demonstrated to directly contribute to the process of several diseases [50]. TLRs interact with endogenous molecules released from damaged tissues or dead cells and regulate many inflammation processes. Endogenous TLR ligands are a group of molecules derived from host tissues or cells, either components of cells or induced gene products in specific conditions. In pathological conditions, endogenous ligands are either released passively from injured/inflamed tissues and dying cells or actively secreted by activated cells [51].

Here, our results revealed that RA inhibited the activation of TLR4, suggesting that the TLR4-mediated NF-κB and STAT3 pathway could be responsible for tumor load reduction demonstrated by RA in the

AOM/DSS-induced CRC mouse model. In addition, to confirm the anti-tumor property of RA, we developed a CM culture system in which colon cancer cells were exposed to CM from PMA-stimulated THP-1 cells, wherein THP-1 monocytes underwent differentiation to macrophages using PMA. Establishing inflammatory conditions in tumor microenvironments provides crosstalk between macrophages and tumor cells as well as facilitates angiogenesis, tumor cell motility, and tumor cell metastasis [52]. Consistent with this hypothesis, several studies have reported that tumor-associated macrophage (TAM) is a key mediator of the connection between inflammation and cancer [4]. A previous study also reported that macrophage CM induced the migration of colon cancer cells and suggested that a TAM-enriched tumor microenvironment promotes cancer cell progression via various mediators [53]. Zhou Y. et al reported that THP-1-CM induces the production of pro-inflammatory cytokines and activation of NF-κB and STAT3 signaling as much as the LPS treatment in gastric cancer cells [54]. AG490, a specific and potent inhibitor of JAK2, was used as a positive control

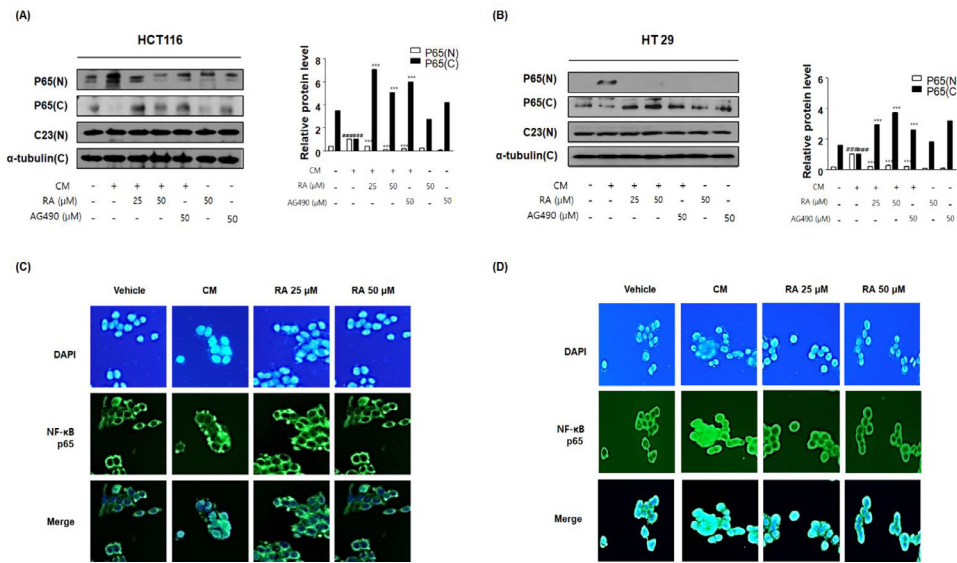


Fig. 7. Effect of RA on NF- κ B activation in human colon cancer cells exposed to inflammatory microenvironments. Every group was treated with CM. In the conditioned culture system, the ratio of the colon cancer cell media to the THP-1 supernatant was 1:5. The vehicle groups were treated with CM from the non-stimulated THP-1 cell group. The cells exposed to CM from PMA-activated THP-1 cells received no treatment or were treated with 25 and 50 μ M RA and 50 μ M AG 490, and the cells were incubated for an additional 30 min. (A, B) NF- κ B p65 translocation to the nucleus was estimated by western blotting in triplicate. Total protein extracts and nuclear and cytosol extracts were prepared from HCT116 and HT29 cells. C23, α -tubulin, and β -actin were used as internal controls. Values are presented as means \pm standard deviations; ### $P < 0.001$ vs the vehicle group; *** $P < 0.001$ vs CM from PMA-activated THP-1 cell-treated group; significances between groups were determined by analysis of variance and Dunnett's post hoc test. (C-D) Immunofluorescence staining of NF- κ B p65 (green) and 4'6-diamidino-2-phenylindole (DAPI; blue) in CM-treated (C) HCT116 and (D) HT29 cells treated with or without RA25 and 50 μ M.

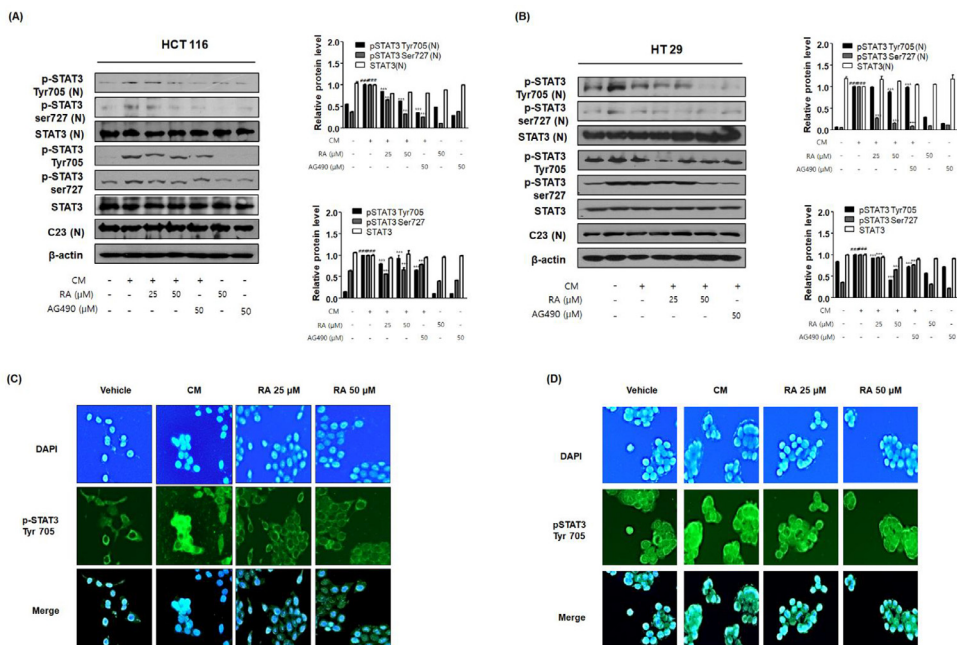


Fig. 8. Effect of RA on STAT3 activation in human colon cancer cells exposed to inflammatory microenvironments. HCT116 and HT29 cells exposed to CM received no treatment or were treated with 25, 50 μ M RA or 50 μ M AG 490, and the cells were further incubated for 30 min. (A, B) The expression of pSTAT3 and translocation to the nucleus were estimated by western blotting in triplicate. C23 and β -actin were used as internal controls. Total protein extracts and nuclear and cytosol extracts were prepared from HCT116 and HT29 cells. Values are presented as means \pm standard deviations; ### $P < 0.001$ vs the vehicle group; *** $P < 0.001$ vs the CM from the PMA-activated THP-1 cells treated group; significances between treated groups were determined using an analysis of variance and Dunnett's post hoc test. (C-D) Immunofluorescence staining of pSTAT3 Tyr 705 (green) and 4'6-diamidino-2-phenylindole (DAPI; blue) in CM-treated (C) HCT116 and (D) HT29 cells treated with or without RA 25 and 50 μ M. Note that the merged regions indicate the co-localization of the target molecules in the bottom panels.

to evaluate the inhibitory effect of RA via TLR-4 mediated NF- κ B/STAT3 pathways. It has been established that JAK2 has considerable effects on TLR-mediated biological responses to LPS in macrophages [55]. In the present study, interestingly, we confirmed that CM promotes TLR4-mediated NF- κ B and STAT3 activation and that RA and AG490 treatments remarkably inhibited phosphorylation and nuclear translocation of NF- κ B and STAT3.

One question pertaining to our results that remains unclear is regarding the specific mediators within CM that are directly associated with the activation of transcription factors in inflammatory tumor microenvironments. Future studies could investigate the detailed mechanisms involved in these processes; however, our study provided evidence that RA remarkably repressed tumor burden and suppressed the progression of adenomas in AOM/DSS-induced CAC mice via the inhibition of TLR4-mediated NF- κ B and STAT3 activation. Moreover, we performed *in vitro* experiments to demonstrate the proposed effect of RA on the inhibition of TLR4-MD-2 binding and NF- κ B and STAT3 in a macrophage CM-treated colon cancer cell line. As an extension to our previous data focused on the manner in which RA suppressed DSS-induced colitis, our present findings provide mechanistic evidence that RA can prevent the development and progression of CAC as a natural compound-based chemopreventive agent.

The purpose of this study was to investigate the therapeutic effects of RA and the mechanisms underlying these effects. The evidence from this study suggests that RA is a considerably potent anti-tumor candidate for CAC. To the best of our knowledge, this is the first study that has documented the competitive inhibition of the TLR4-MD-2 complex by RA. As a result, RA treatment suppressed TLR4-mediated NF- κ B and STAT3 activation in the AOM/DSS-induced CAC murine model and abrogated the progression of colon cancer cells in an inflammation-relative microenvironment.

Competing interest

The authors declare no conflict of interest.

Data sharing statement

The data that support the findings of this study are available from the corresponding author upon reasonable request.

Author contributions

B.-R.J., K.-S.C., and H.-J.A. conceived and designed the experiments. B.-R.J., S.-J.H., S.-N.H., and M.L. performed the experiments and B.-R.J. analyzed the data with K.-S.C., K.-J.L., M.L., H.-J.A., M.L., and H.-J.A. contributed reagents, materials, and analysis tools. B.-R.J., M.L., and H.-J.A. wrote the paper. All authors read and approved the final manuscript.

Funding

This study was supported by the NRF (National Research Foundation of Korea) Grant funded by the Korean Government (NRF-2017R1C1B2008617, NRF-2017M3A9B6061511 and NRF-2018-Fostering Core Leaders of the Future Basic Science Program/Global Ph.D. Fellowship Program).

References

- [1] Siegel RL, Miller KD, Jemal A. Cancer statistics, 2016. *CA: a cancer j for clin* 2016;**66**:7–30.
- [2] Eaden J, Abrams K, McKay H, Denley H, Mayberry J. Inter-observer variation between general and specialist gastrointestinal pathologists when grading dysplasia in ulcerative colitis. *The J pathol* 2001;**194**:152–7.
- [3] Nadeem MS, Kumar V, Al-Abbasi FA, Kamal MA, Anwar F. Risk of colorectal cancer in inflammatory bowel diseases. *Seminars in cancer biology* 64, 51–60.
- [4] Sica A, Allavena P, Mantovani A. Cancer related inflammation: the macrophage connection. *Cancer Lett* 2008;**267**:204–15.
- [5] Keibel A, Singh V, Sharma MC. Inflammation, microenvironment, and the immune system in cancer progression. *Curr Pharm Des* 2009;**15**:1949–55.
- [6] Fukata M, Shang L, Santaolalla R, Sotolongo J, Pastorini C, Espana C, Ungaro R, Harpaz N, Cooper HS, Elson G, et al. Constitutive activation of epithelial TLR4 augments inflammatory responses to mucosal injury and drives colitis-associated tumorigenesis. *Inflammatory bowel dis* 2011;**17**:1464–73.
- [7] Huang HY, Zhang ZJ, Cao CB, Wang N, Liu FF, Peng JQ, Ren XJ, Qian J. The TLR4/NF-kappaB signaling pathway mediates the growth of colon cancer. *Euro rev for med and pharmacol sci* 2014;**18**:3834–43.
- [8] Multhoff G, Molls M, Radons J. Chronic inflammation in cancer development. *Frontiers in immunol* 2011;**2**:98.
- [9] Liu BS, Cao Y, Huizinga TW, Hafler DA, Toes RE. TLR-mediated STAT3 and ERK activation controls IL-10 secretion by human B cells. *Eur j immunol* 2014;**44**:2121–9.
- [10] Pandurangan AK, Esa NM. Signal transducer and activator of transcription 3 - a promising target in colitis-associated cancer. *Asian Pacific j cancer prevention: APJCP* 2014;**15**:551–60.
- [11] Amoah SK, Sandjo LP, Kratz JM, Biavatti MW. Rosmarinic acid—pharmaceutical and clinical aspects. *Planta Med* 2016;**82**:388–406.
- [12] Yoshida M, Fuchigami M, Nagao T, Okabe H, Matsunaga K, Takata J, Karube Y, Tsuchihashi R, Kinjo J, Mihashi K, et al. Antiproliferative constituents from Umbelliferae plants VII. Active triterpenes and rosmarinic acid from *Centella asiatica*. *Biol & pharmaceutical bulletin* 2005;**28**:173–5.
- [13] Anusuya C, Manoharan S. Antitumor initiating potential of rosmarinic acid in 7,12-dimethylbenz(a)anthracene-induced hamster buccal pouch carcinogenesis. *J environmental pathol, toxicol and oncol: off organ of the Int Soc for Environmental Toxicol and Cancer* 2011;**30**:199–211.
- [14] Zhang Y, Chen X, Yang L, Zu Y, Lu Q. Effects of rosmarinic acid on liver and kidney antioxidant enzymes, lipid peroxidation and tissue ultrastructure in aging mice. *Food & function* 2015;**6**:927–31.
- [15] Chockalingam N, Muruhan S. Anti-inflammatory properties of rosmarinic acid—a review. *Int J Res in Pharmaceutical Sci* 2017;**8**:656–62.
- [16] Jin BR, Chung KS, Cheon SY, Lee M, Hwang S, Noh Hwang S, Rhee KJ, An HJ. Rosmarinic acid suppresses colonic inflammation in dextran sulphate sodium (DSS)-induced mice via dual inhibition of NF-kappaB and STAT3 activation. *Scientific rep* 2017;**7**:46252.
- [17] Karthikkumar V, Sivagami G, Vinothkumar R, Rajkumar D, Nalini N. Modulatory efficacy of rosmarinic acid on premalignant lesions and antioxidant status in 1,2-dimethylhydrazine induced rat colon carcinogenesis. *Environmental toxicol and pharmacol* 2012;**34**:949–58.
- [18] Rhee KJ, Wu S, Wu X, Huso DL, Karim B, Franco AA, Rabizadeh S, Golub JE, Mathews LE, Shin J, et al. Induction of persistent colitis by a human commensal, enterotoxigenic *Bacteroides fragilis*, in wild-type C57BL/6 mice. *Infect Immun* 2009;**77**:1708–18.
- [19] Chung KS, Cheon SY, Roh SS, Lee M, An HJ. Chemopreventive Effect of *Aster glehni* on Inflammation-Induced Colorectal Carcinogenesis in Mice. *Nutrients* 2018;**10**.
- [20] Trott O, Olson AJ. AutoDock Vina: improving the speed and accuracy of docking with a new scoring function, efficient optimization, and multithreading. *J Comput Chem* 2010;**31**:455–61.
- [21] Kim HM, Park BS, Kim JI, Kim SE, Lee J, Oh SC, Enkhbayar P, Matsushima N, Lee H, Yoo OJ, et al. Crystal structure of the TLR4-MD-2 complex with bound endotoxin antagonist Eritoran. *Cell* 2007;**130**:906–17.
- [22] DeLano WL. Pymol: An open-source molecular graphics tool. *CCP4 Newsletter On Protein Crystallography* 2002;**40**:82–92.
- [23] Wallace AC, Laskowski RA, Thornton JM. LIGPLOT: a program to generate schematic diagrams of protein-ligand interactions. *Protein Eng* 1995;**8**:127–34.
- [24] De Robertis M, Massi E, Poeta ML, Carotti S, Morini S, Cecchetelli L, Signori E, Fazio VM. The AOM/DSS murine model for the study of colon carcinogenesis: From pathways to diagnosis and therapy studies. *J carcinogenesis* 2011;**10**:9.

- [25] Biton IE, Stettner N, Brener O, Erez A, Harmelin A, Garbow JR. Assessing mucosal inflammation in a DSS-induced colitis mouse model by MR colonography. *Tomography* 2018;**4**:4–13.
- [26] Sun Q, Liu Q, Zheng Y, Cao X. Rapamycin suppresses TLR4-triggered IL-6 and PGE(2) production of colon cancer cells by inhibiting TLR4 expression and NF-kappaB activation. *Molecular immunol* 2008;**45**:2929–36.
- [27] Zhou L, Liang H-Z, Zhang H, Wang X-Y, Xu D, Wu J (2018). Significance of TLR4, MyD88 and STAT3 expression in colorectal cancer.
- [28] Cochet F, Facchini FA, Zaffaroni L, Billod JM, Coelho H, Holgado A, Braun H, Beyaert R, Jerala R, Jimenez-Barbero J, et al. Novel carboxylate-based glycolipids: TLR4 antagonism, MD-2 binding and self-assembly properties. *Scientific rep* 2019;**9**:919.
- [29] Aggarwal BB, Vijayalekshmi RV, Sung B. Targeting inflammatory pathways for prevention and therapy of cancer: short-term friend, long-term foe. *Clin cancer res: an off J Am Assoc for Cancer Res* 2009;**15**:425–30.
- [30] Lasry A, Zinger A, Ben-Neriah Y. Inflammatory networks underlying colorectal cancer. *Nature Immunol* 2016;**17**:230–40.
- [31] Hussain SP, Harris CC. Inflammation and cancer: an ancient link with novel potentials. *Int J Cancer* 2007;**121**:2373–80.
- [32] Itzkowitz SH, Yio X. Inflammation and cancer IV. Colorectal cancer in inflammatory bowel disease: the role of inflammation. *Am J physiol Gastrointestinal and liver physiol* 2004;**287**:G7–17.
- [33] Burn J, Gerdes AM, Macrae F, Mecklin JP, Moeslein G, Olschwang S, Eccles D, Evans DG, Maher ER, Bertario L, et al. Long-term effect of aspirin on cancer risk in carriers of hereditary colorectal cancer: an analysis from the CAPP2 randomised controlled trial. *Lancet* 2011;**378**:2081–7.
- [34] Chung KS, Choi HE, Shin JS, Cho EJ, Cho YW, Choi JH, Baek NI, Lee KT. Chemopreventive effects of standardized ethanol extract from the aerial parts of *Artemisia princeps* Pampanini cv. Sajabal via NF-kappaB inactivation on colitis-associated colon tumorigenesis in mice. *Food and chemical toxicol: an int J published for the Br Industrial Biol Res Assoc* 2015;**75**:14–23.
- [35] Qiu X, Ma J, Wang K, Zhang H. Chemopreventive effects of 5-aminosalicylic acid on inflammatory bowel disease-associated colorectal cancer and dysplasia: a systematic review with meta-analysis. *Oncotarget* 2017;**8**:1031–45.
- [36] Cohen HD, Das KM. The metabolism of mesalamine and its possible use in colonic diverticulitis as an anti-inflammatory agent. *J clin gastroenterol* 2006;**40**(Suppl 3):S150–4.
- [37] Cunningham D, Maroun J, Vanhoefer U, Van Cutsem E. Optimizing the use of irinotecan in colorectal cancer. *The oncol* 2001;**6**(Suppl 4):17–23.
- [38] MacDonald V. Chemotherapy: managing side effects and safe handling. *The Canadian veterinary J = La revue veterinaire canadienne* 2009;**50**:665–8.
- [39] Schmoll HJ, Arnold D. Update on capecitabine in colorectal cancer. *The oncol* 2006;**11**:1003–9.
- [40] Tanaka T, Kohno H, Suzuki R, Yamada Y, Sugie S, Mori H. A novel inflammation-related mouse colon carcinogenesis model induced by azoxymethane and dextran sodium sulfate. *Cancer sci* 2003;**94**:965–73.
- [41] Rubin DC, Shaker A, Levin MS. Chronic intestinal inflammation: inflammatory bowel disease and colitis-associated colon cancer. *Frontiers in immunol* 2012;**3**:107.
- [42] Baud V, Karin M. Is NF-kappaB a good target for cancer therapy? Hopes and pitfalls. *Nature rev Drug discovery* 2009;**8**:33–40.
- [43] Karin M, Lin A. NF-kappaB at the crossroads of life and death. *Nature immunol* 2002;**3**:221–7.
- [44] Verzella D, Pescatore A, Capece D, Vecchiotti D, Ursini MV, Franzoso G, Alesse E, Zazzeroni F. Life, death, and autophagy in cancer: NF-kappaB turns up everywhere. *Cell death & dis* 2020;**11**:210.
- [45] Wang SW, Sun YM. The IL-6/JAK/STAT3 pathway: potential therapeutic strategies in treating colorectal cancer (Review). *Int J Oncol* 2014;**44**:1032–40.
- [46] Xin-hua B, Rui-yu L. Progress in research on correlation among STAT3, CyclinD1, P21 genes and tumors. *Journal of Otol* 2012;**7**:19–24.
- [47] Fukata M, Hernandez Y, Conduah D, Cohen J, Chen A, Breglio K, Goo T, Hsu D, Xu R, Abreu MT. Innate immune signaling by Toll-like receptor-4 (TLR4) shapes the inflammatory microenvironment in colitis-associated tumors. *Inflammatory bowel dis* 2009;**15**:997–1006.
- [48] So EY, Ouchi T. The application of Toll like receptors for cancer therapy. *Int J biol sci* 2010;**6**:675–81.
- [49] Greenhill CJ, Rose-John S, Lissilaa R, Ferlin W, Ernst M, Hertzog PJ, Mansell A, Jenkins BJ. IL-6 trans-signaling modulates TLR4-dependent inflammatory responses via STAT3. *J Immunol* 2011;**186**:1199–208.
- [50] Molteni M, Gemma S, Rossetti C. The role of toll-like receptor 4 in infectious and noninfectious inflammation. *Mediators Inflamm* 2016;**2016**.
- [51] Yu L, Wang L, Chen S. Endogenous toll-like receptor ligands and their biological significance. *J cellular and molecular med* 2010;**14**:2592–603.
- [52] Condeelis J, Pollard JW. Macrophages: obligate partners for tumor cell migration, invasion, and metastasis. *Cell* 2006;**124**:263–6.
- [53] Zhang Y, Sime W, Juhas M, Sjolander A. Crosstalk between colon cancer cells and macrophages via inflammatory mediators and CD47 promotes tumour cell migration. *Eur J cancer* 2013;**49**:3320–34.
- [54] Zhou Y, Xia L, Liu Q, Wang H, Lin J, Oyang L, Chen X, Luo X, Tan S, Tian Y, et al. Induction of Pro-Inflammatory Response via Activated Macrophage-Mediated NF-kappaB and STAT3 Pathways in Gastric Cancer Cells. *Cellular physiol and biochemistry: int j experimental cellular physiology, biochemistry, and pharmacol* 2018;**47**:1399–410.
- [55] Okugawa S, Ota Y, Kitazawa T, Nakayama K, Yanagimoto S, Tsukada K, Kawada M, Kimura S. Janus kinase 2 is involved in lipopolysaccharide-induced activation of macrophages. *Am J physiol Cell physiol* 2003;**285**:C399–408.